The *a*3 isoform of V-ATPase regulates insulin secretion from pancreatic β-cells

Ge-Hong Sun-Wada[1,*], Takao Toyomura[2], Yoshiko Murata[2], Akitsugu Yamamoto[3], Masamitsu Futai[4] and Yoh Wada[2]

[1]Department of Biochemistry, Faculty of Pharmaceutical Sciences, Doshisha Women's College, Kyotanabe 610-0395, Japan
[2]Division of Biological Sciences, Institute of Scientific and Industrial Research, Osaka University, Osaka 567-0047, Japan
[3]Nagahama Institute of Bio-Science and Technology, Nagahama 526-0829, Japan
[4]Futai Special Laboratory, Microbial Chemistry Research Center, CREST, Japan Science and Technology Agency, Tokyo 141-0021, Japan
*Author for correspondence (e-mail: kwada@dwc.doshisha.ac.jp)

Accepted 30 August 2006
Journal of Cell Science 119, 4531-4540 Published by The Company of Biologists 2006
doi:10.1242/jcs.03234

Summary

Vacuolar-type H^+-ATPase (V-ATPase) is a multi-subunit enzyme that has important roles in the acidification of a variety of intracellular compartments and some extracellular milieus. Four isoforms for the membrane-intrinsic subunit (subunit *a*) of the V-ATPase have been identified in mammals, and they confer distinct cellular localizations and activities on the proton pump. We found that V-ATPase with the *a*3 isoform is highly expressed in pancreatic islets, and is localized to membranes of insulin-containing secretory granules in β-cells. *oc/oc* mice, which have a null mutation at the *a*3 locus, exhibited a reduced level of insulin in the blood, even with high glucose administration. However, islet lysates contained mature insulin, and the ratio of the amount of insulin to proinsulin in *oc/oc* islets was similar to that of wild-type islets, indicating that processing of insulin was normal even in the absence of the *a*3 function. The insulin contents of *oc/oc* islets were reduced slightly, but this was not significant enough to explain the reduced levels of the blood insulin. The secretion of insulin from isolated islets in response to glucose or depolarizing stimulation was impaired. These results suggest that the *a*3 isoform of V-ATPase has a regulatory function in the exocytosis of insulin secretion.

Key words: V-ATPase, Insulin secretion, Exocytosis, *a*3 isoform, Mouse mutant

Introduction

Maintenance of a luminal acidic environment in the exocytic and endocytic pathways is required at various stages in the processing and sorting of vesicle contents for a variety of signaling molecules, secretory and surface proteins, and ligand-receptor complexes (Futai et al., 2000; Weisz, 2003). The secretory granules have a luminal pH of 5.0-5.5 (Arvan and Castle, 1986; Orci et al., 1986; Urbe et al., 1997), and their acidification has important roles in the condensation and maturation of their contents (Hutton, 1994). The electrochemical proton gradient across the membrane provides the energy for accumulation of neurotransmitters into synaptic vesicles (Moriyama and Futai, 1990; Nelson, 1993). Many growth factors are produced as latent inactive forms within the endoplasmic reticulum and undergo several modifications during travel through the Golgi apparatus, before being converted to mature active forms within the secretory vesicles. For instance, processing of insulin from proinsulin initiates in clathrin-coated secretory vesicles (Orci et al., 1987) by the activities of two enzymes, PC2 and PC3. Because PC3 shows a strict pH dependence (Orci et al., 1994; Smeekens et al., 1992), the acidification inside the secretory vesicles has fundamental importance for maintenance of whole-body homeostasis. It has been suggested for decades that the proton gradients might be involved in the fusion of secretory vesicles to the target membrane (Al-Awqati, 1986; Burgess and Kelly, 1987). Barg et al. showed that the acidic pH might regulate priming of the granules for secretion, a process involving pairing of SNARE proteins on the vesicles and target membranes to establish fusion competence (Barg et al., 2001).

Recently, several lines of evidence indicated that the membrane fusion events are regulated by a proton-pumping vacuolar-type ATPase (V-ATPase), which is the key enzyme acidifying a wide variety of intracellular compartments and some extracellular milieus. V-ATPase is a multi-subunit complex that comprises two major functional sectors known as V_1 and V_O. The V_1 sector is involved in ATP hydrolysis and consists of eight subunits (*A*, *B*, *C*, *D*, *E*, *F*, *G* and *H*) (for reviews, see Futai et al., 2000; Nelson and Harvey, 1999; Nishi and Forgac, 2002; Sun-Wada et al., 2003). The V_O sector consists of up to 6 subunits (*a*, *c*, *c′*, *c″ d* and *e*) and forms a proton pathway (Anraku, 1996). In yeast vacuolar fusion, this membrane-intrinsic sector has been demonstrated to be an essential component (Peters et al., 2001). Interaction between the SNARE complex and the V_O sector has been shown in *Torpedo* nerve terminals (Morel et al., 2003). Most recently, Hiesinger et al. demonstrated genetically and electrophysiologically that the *Drosophila* V-ATPase *a* subunit has a regulatory function in a late step of synaptic vesicle exocytosis (Hiesinger et al., 2005). Mutant *Caenorhabditis elegans* with a mutation at V_O subunit *e* (*fus-1*) or *C. elegans* with impaired V-ATPase function induced by RNA interference (RNAi) exhibit hyperactive cell-cell fusion (Kontani et al., 2005). These results are highly indicative that the V-ATPase is directly or indirectly involved in dynamic membrane interaction, including vesicle transport or cell-cell

fusion. However, the precise molecular mechanism as to how V-ATPase regulates the membrane dynamics remains to be elucidated.

We noted that endocrine cells might be a good system to explore V-ATPase function in regulated secretion: hormones to be secreted undergo sequential post-translational modifications that are thought to be dependent on luminal acidification, and vesicle fusion or hormone release are triggered by external or internal stimuli. In this study, we focused on the insulin-containing secretory granules in pancreatic β-cells. Previous studies suggested that the V-ATPase function might be important for the appropriate processing and maturation of insulin (Hutton, 1994; Orci et al., 1994; Orci et al., 1986; Smeekens et al., 1992). However, a mutant mouse with defective V-ATPase subunits in their secretory vesicles could produce the mature active insulin, whereas the mutant was less competent for hormone secretion following stimulation both in vivo and in vitro. These results indicate that the *a*3 isoform of V-ATPase has a regulatory role in the secretion of insulin-containing granules.

Results

Expression and localization of *a* subunit isoforms in mouse pancreas

The V-ATPases in mammals, nematodes and flies exhibit structural and functional diversities as most of their subunits are not coded by a single gene but instead by multiple genes with distinctive structure. For the V_O membrane-intrinsic sector, only single genes for the small, highly hydrophobic 16 kDa and 23 kDa subunits are functional in mammals (Hayami et al., 2001; Sun-Wada et al., 2001; Sun-Wada et al., 2000). The *a* subunit is a protein with a relative molecular mass of approximately 100 kDa, with an N-terminal cytosolic portion and 9 membrane-spanning segments (Futai et al., 2000; Nelson and Harvey, 1999; Nishi and Forgac, 2002; Sun-Wada et al., 2003). In mammalian cells, four isoforms of the *a* subunit (*a*1, *a*2, *a*3 and *a*4) have been identified (Nishi and Forgac, 2000; Oka et al., 2001; Smith et al., 2001; Toyomura et al., 2000). We have previously shown that the *a*1, *a*2 and *a*3 isoforms are expressed ubiquitously in mouse tissues (Toyomura et al., 2000) and exhibit distinct cellular localizations (Toyomura et al., 2003). The *a*4 isoforms is unique, as its expression is restricted to kidney (Oka et al., 2001; Smith et al., 2001).

In these studies, we noted that the pancreas accumulates significant amounts of mRNA of the *a*3 isoform, as well as the *a*3 isoform itself. We examined the distribution of the *a*1, *a*2 and *a*3 isoforms in mouse pancreas using isoform-specific antibodies (Toyomura et al., 2000) (Fig. 1A-D). A strong signal of the *a*3 isoform was detected in almost all the cells in the islets of Langerhans (Fig. 1D). The *a*3 isoform accumulated less in the surrounding pancreatic acini. The signals of *a*1 and *a*2 in the islet region were similar to signals in the surrounding tissues (Fig. 1B,C). The insulin-secreting β-cells make up about 70% of the islet, whereas the glucagon-secreting α-cells constitute some 20% of the islet and tend to be distributed towards the periphery (Fig. 2). Immunostaining of serial sections of the islet with anti-*a*3, anti-insulin and anti-glucagon antibodies revealed that the *a*3 isoform exhibited high expression in almost all the islet cells, including β, α and other islet cells (Fig. 2).

Next, we analyzed the cellular localization of *a*3 in two β-cell lines, βTC6 (Poitout et al., 1995) and βHC9 (Noda et al., 1996; Radvanyi et al., 1993), which were established from genetically modified mice transgenic for SV40 large T antigen (Noda et al., 1996; Poitout et al., 1995; Radvanyi et al., 1993). These cell lines preserve some distinctive characteristics of β-cells, including glucose-inducible insulin secretion, and thus provide a model system for dissecting the molecular mechanisms of regulated secretion (Noda et al., 1996; Poitout et al., 1995; Radvanyi et al., 1993). In βTC6 cells, the *a*3 signal nearly completely overlapped that of insulin (Fig. 3A), suggesting that *a*3 is localized to secretory granules containing insulin. Another class of secretory vesicles called synaptic-like microvesicles (SLMVs) in β-cells accumulate γ-amino butyric acid (GABA), but not insulin (Moriyama et al., 1996). SLMVs are stained by synaptophysin (Hayashi et al., 1998) as shown in Fig. 3. However, the synaptophysin-positive compartments did not possess the *a*3 isoform, suggesting that the *a*3 isoform is preferentially localized to the insulin-containing secretory vesicles. The *a*3 signals did not overlap with those of other organelle marker proteins, including lysosome-associated membrane protein 2 (lamp-2; in lysosomes and late endosomes) (Granger et al., 1990; Uthayakumar et al., 1990) and GM130 (in cis-Golgi) (Nakamura et al., 1997) (Fig. 3). It is noteworthy that the *a*3 isoform is a resident of lysosomes and late endosomes in fibroblastic NIH3T3 cells or undifferentiated RAW 264.7 cells (Toyomura et al., 2003). Similar results were obtained with βHC9 cells (Fig. 3B). We found that the *a*3 isoform signal exhibited good merging with that of insulin, whereas *a*1 and *a*2 showed different localizations in βHC9 cells.

We further assessed localization of the *a*3 isoform using

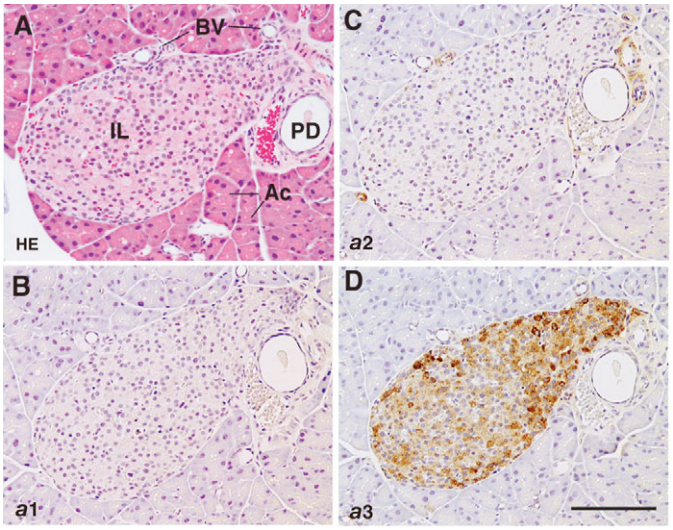

Fig. 1. Localization of *a* subunit isoforms in the islet of Langerhans. (A-D) Serial paraffin sections of a pancreatic islet were stained with hematoxylin and eosin (A, HE), and anti-*a*1 (B), anti-*a*2 (C) and anti-*a*3 (D) antibodies. IL, islet of Langerhans; BV, blood vessel; Ac, acini; PD, pancreatic duct. Strong signals of the *a*3 isoform were detected in almost all the cells in the islet of Langerhans. Strong signals of the *a*2 isoform were also detected in the epithelial cells of blood vessels (A and C). Bar, 100 μm.

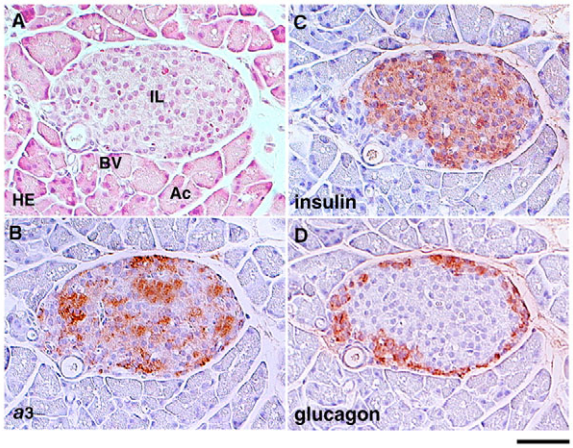

Fig. 2. Serial paraffin sections of a pancreatic islet were stained with hematoxylin and eosin (A, HE), and anti-*a*3 (B), anti-insulin (C) and anti-glucagon (D) antibodies. IL, islet of Langerhans; BV, blood vessel; Ac, acini. Bar, 50 μm.

immunoelectron microscopy. A substantial amount of the anti-*a*3 labeling was associated with vesicles containing electron-dense cores, which is typical morphology of insulin-containing secretory granules (Fig. 4A). The *a*3 labeling was found on the limiting membranes of the vesicles. We quantified the labeling by counting gold particles and found that over 80% of total gold particles were distributed in the vesicles with a dense core, whereas fewer than 5% of the particles were found in Golgi and late endosome/lysosomes (multi-vesicular bodies) (Fig. 4B). From these immunohistological observations at tissue and ultra-structural levels, we concluded that the *a*3 isoform is expressed in mouse β-cells, and is preferentially localized in secretory vesicles containing insulin.

Expression of *a*3 in pancreatic islets of *oc/oc* mutant mice

Osteosclerosis (*oc*) is an autosomal recessive mutation that impairs bone resorption by osteoclasts and induces a general increase in bone density in affected mice (Schlager and Dickie, 1967; Scimeca et al., 2000). *oc*/*oc* homozygous mice survive for 4 weeks after birth, but begin to die around the weaning period. The *oc* mutation comprises a 1.6 kb deletion in the *a*3 subunit locus, which is involved in translation initiation (Scimeca et al., 2000). Loss of the *a*3 subunit results in a lack of V-ATPase in the membranes of osteoclast cells, thereby preventing bone resorption (Scimeca et al., 2000). Considering the large amount of accumulation of the *a*3 isoform in the insulin-containing granules, we expected that *oc*/*oc* mutants might develop metabolic disorders owing to endocrine dysfunction, although little has been described on pancreatic function in *oc*/*oc* mice.

We examined protein levels of the V-ATPase *a*3 isoform by immunoblotting pancreas lysates using specific antibodies. The *a*3 isoform was not present in *oc*/*oc* pancreatic lysates, as expected from the fact that the mutation deletes the translation initiation codon and its surrounding region; thus, *oc* probably represents a null mutation. The *a*1 and *a*2 isoforms were present, as shown in Fig. 5. Interestingly, the level of *a*2 was slightly elevated in the mutant mice compared with in the wild-type mice, suggesting that some compensating mechanisms might exist to maintain the cellular amounts of the V-ATPase complex. The slight elevation of the *a*2 isoform in the *oc*/*oc* mutant was also confirmed using total lysates prepared from pancreatic islets (Fig. 5B). The localization of the *a*2 isoform in *oc*/*oc* β-cells was further examined by immunofluorescence staining. We found that the *a*2 signals were diffused and overlapped with that of insulin; whereas, the *a*2 signals were more concentrated in the perinuclear region in wild-type cells (Fig. 5C).

The morphology of the islets and the immunostaining intensity of insulin in the mutant mice were indistinguishable from those in the wild-type mice (Fig. 6A). Although reduction of islet size is often associated with islet cell abnormalities (Unno et al., 2002), no reduced β-cell mass was observed in *oc*/*oc* mice, indicating that differentiation/proliferation of β-cells was not affected by the loss of the *a*3 isoform. The lack of expression of the *a*3 isoform in *oc*/*oc* islets was also confirmed using serial sections (Fig. 6A, lower panels). The morphology of the secretory granules was examined using electron microscopy. Secretory vesicles with a dense core were observed both in *oc*/*oc* and wild-type islets (Fig. 6B). We also measured the density of the secretory vesicles. There was no significant difference observed in the density of wild-type [148.5±8.9 (arbitrary unit), n=60] and *oc*/*oc* insulin granules (147.1±10.2, n=73, P>0.3, compared with wild-type granules).

Processing of insulin in the islets of *oc*/*oc* mice

Because the conversion of proinsulin to insulin is strictly dependent on a low pH (Orci et al., 1994; Smeekens et al., 1992), we presumed that loss of the V-ATPase *a*3 isoform would result in abnormal luminal acidification, and thereby affect insulin processing and maturation. Insulin processing was examined using immunoblotting analysis of isolated islets. The insulin migrated to 3.5 kDa (separated A and B chains on a reducing gel) close to the position of human insulin in both the wild-type and *oc*/*oc* mice (Fig. 7, lanes 1, 2 and 3, arrows). The anti-insulin antibody, which recognizes proinsulin as well, detected the 7.6 kDa proinsulin form in both the normal and mutant islets (Fig. 7, lanes 2 and 3, arrows). The amounts of insulin and proinsulin decreased in the islets of *oc*/*oc* mice, consistent with the results of insulin content in islets determined by enzyme-linked immunosorbent assay (ELISA). Imunoblotting with anti-C-peptide also revealed the 7.6 kDa protein in both the wild-type and *oc*/*oc* mice (Fig. 7, lanes 4 and 5, arrows). The ratios of the level of insulin over proinsulin were 1.74 and 1.63 for wild-type and mutant mice, respectively (Fig. 7). The results indicated that proinsulin was converted to insulin in *oc*/*oc* mice, and no significant accumulation of proinsulin was found in the mutant mice. Furthermore, the lysates of wild-type and *oc*/*oc* pancreas evoked translocation of the GLUT-4 glucose transporter (James et al., 1994) from intracellular compartments to the plasma membrane with almost similar dose responses; thus, the lysates of the mutant pancreas contained a biologically active form of insulin (data not shown). These observations indicated that the processing and maturation of insulin was not compromised even in the absence of the V-ATPase *a*3 subunit isoform, a major proton pump on the insulin-containing secretory granules.

Abnormal plasma insulin level in *oc*/*oc* mice

Blood samples were collected from fasting and non-fasting

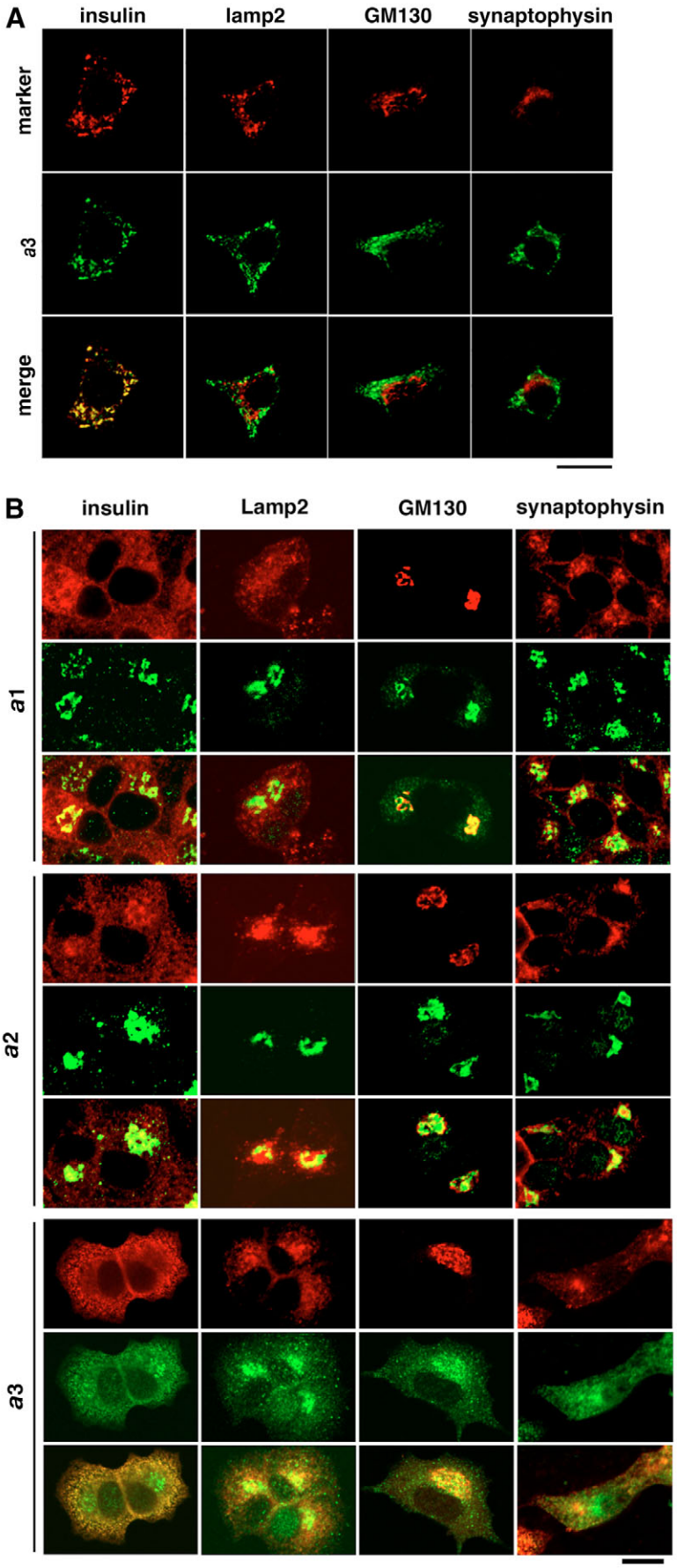

mutant mice, and the blood insulin contents and glucose level were measured (Fig. 8A-C). The plasma insulin level in natural-feeding *oc*/*oc* mice was lower than those in wild-type or heterozygous (*oc*/+) mice (Fig. 8A). Oral glucose administration raised the blood glucose levels in both wild-type, *oc*/+ and *oc*/*oc* mice (Fig. 8C), however, no changes in insulin level were found in *oc*/*oc* mutant mice, whereas the blood insulin level in wild-type and *oc*/+ mice increased (Fig. 8B). These findings indicated that *oc*/*oc* mutant mice were defective in regulating the blood insulin level in response to an increase in the blood glucose level.

Insulin secretion from isolated islets

oc/*oc* mutant mice could produce mature active insulin in pancreatic β-cells but failed to raise the blood insulin level after glucose intake. This phenotype might reflect defective insulin secretion in response to glucose loading in *oc*/*oc* pancreatic β-cells. We prepared islets from wild-type and *oc*/*oc* mice, and measured their secretion activities in the response to glucose or depolarization stimulus. At basal conditions (in the presence of 2.8 mM glucose and 5 mM KCl), insulin secretion of *oc*/*oc* islets was slightly low (Fig. 9A). We found that the insulin content per islet protein in *oc*/*oc* mice was approximately half of that of wild-type mice (Fig. 9B); this reduction might reflect the lower insulin secretion at the basal level. In the presence of 16.7 mM glucose or 60 mM KCl, insulin secretion from the *oc*/*oc* islets was significantly lower than those of the wild-type islets (Fig. 9A), indicating that the mutant islets did not effectively respond to the stimulus and were practically defective in insulin secretion. The localization of the *a*3 subunit did not colocalize with GABA vesicles, which contain synaptophysin as a marker. We have also examined GABA secretion using isolated islets, and no significant difference was observed between wild-type and *oc*/*oc* pancreatic islets (data not shown). Therefore, the secretion defect was specific for insulin.

Granule acidification and insulin secretion

We found that the secretory granules of *oc*/*oc* mutant β-cells were still stained with an acidotropic reagent, LysoTracker, suggesting that the secretory granules without the *a*3 isoform were acidified to a certain degree (Fig. 10A). It is interesting to know whether insulin secretion is dependent on V-ATPase pump activity or on the physical presence of the V-ATPase. We treated βHC9 cells with bafilomycin A,

Fig. 3. Localization of the *a*3 isoform to secretory granules in βTC6 and βHC9 cells. (A) βTC6 cells grown on a slide glass were stained with antibodies against the *a*3 isoform (green), and insulin, lamp-2, GM130, or synaptophysin (red). (B) βHC9 cells were stained with antibodies against the *a* isoforms (*a*1, *a*2 and *a*3, green) and insulin, lamp-2, GM130, or synaptophysin (red). Merged images are also shown. Bar, 10 μm.

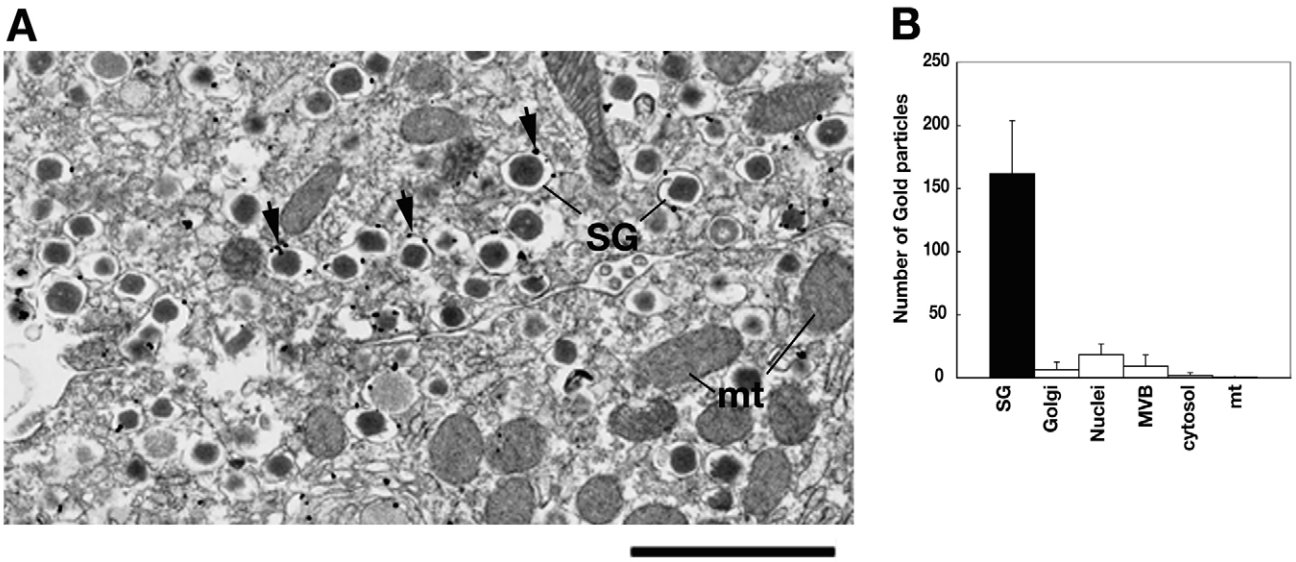

Fig. 4. Localization of the *a*3 isoform in pancreatic β-cells. (A) The localization of *a*3 is shown by electron-dense silver-enhanced immunogold particles (arrows indicate examples): mt, mitochondria; SG, secretory granules. Bar, 1 μm. (B) Quantification of gold particle frequency in secretory granule (SG) or other compartments. Approximately 80% of total gold particles (450 μm^2 × 6 sections, *n*=1193) were distributed in the dense-core granules. MVB, multi-vesicular body; mt, mitochondria.

a specific inhibitor of V-ATPase, and measured the insulin secretion. The acidification of the secretory granules was monitored by LysoTracker staining. We found that the LysoTracker staining was almost absent after treatment with bafilomycin (10 nM) for 1 hour (Fig. 10B), yet the secretion of insulin was not significantly affected (Fig. 10C). These results suggest that the acidification itself is not directly involved in the secretion of existing secretory granules.

Discussion

The *a*3 isoform of V-ATPase is targeted to the membranes of secretory granules

V-ATPases are the most prominent proton pumps functioning in both intracellular and extracellular acidification. They are indispensable for many cellular functions, including receptor-mediated endocytosis, protein processing and degradation. This complex proton pump also generates the proton motive forces across the organelle membranes that are in turn utilized

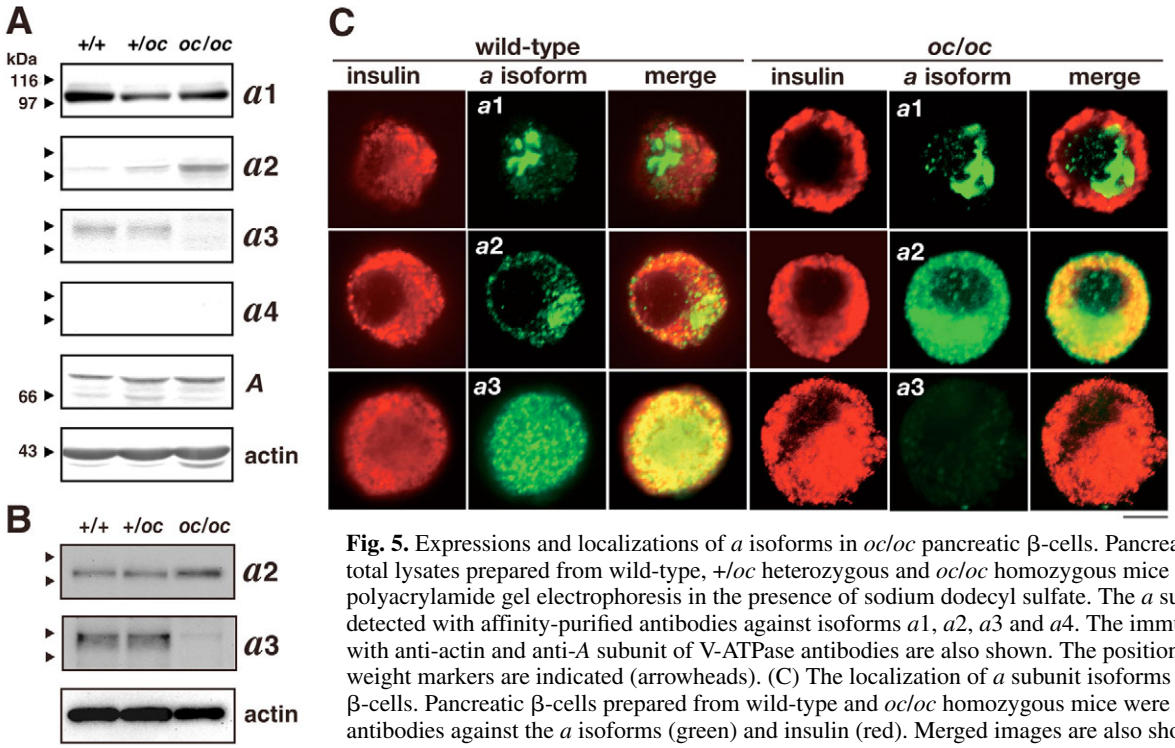

Fig. 5. Expressions and localizations of *a* isoforms in *oc*/*oc* pancreatic β-cells. Pancreas (A) and islet (B) total lysates prepared from wild-type, +/*oc* heterozygous and *oc*/*oc* homozygous mice were subjected to polyacrylamide gel electrophoresis in the presence of sodium dodecyl sulfate. The *a* subunit isoforms were detected with affinity-purified antibodies against isoforms *a*1, *a*2, *a*3 and *a*4. The immunoblots obtained with anti-actin and anti-*A* subunit of V-ATPase antibodies are also shown. The positions of molecular weight markers are indicated (arrowheads). (C) The localization of *a* subunit isoforms in *oc*/*oc* pancreatic β-cells. Pancreatic β-cells prepared from wild-type and *oc*/*oc* homozygous mice were stained with antibodies against the *a* isoforms (green) and insulin (red). Merged images are also shown. Bar, 5 μm.

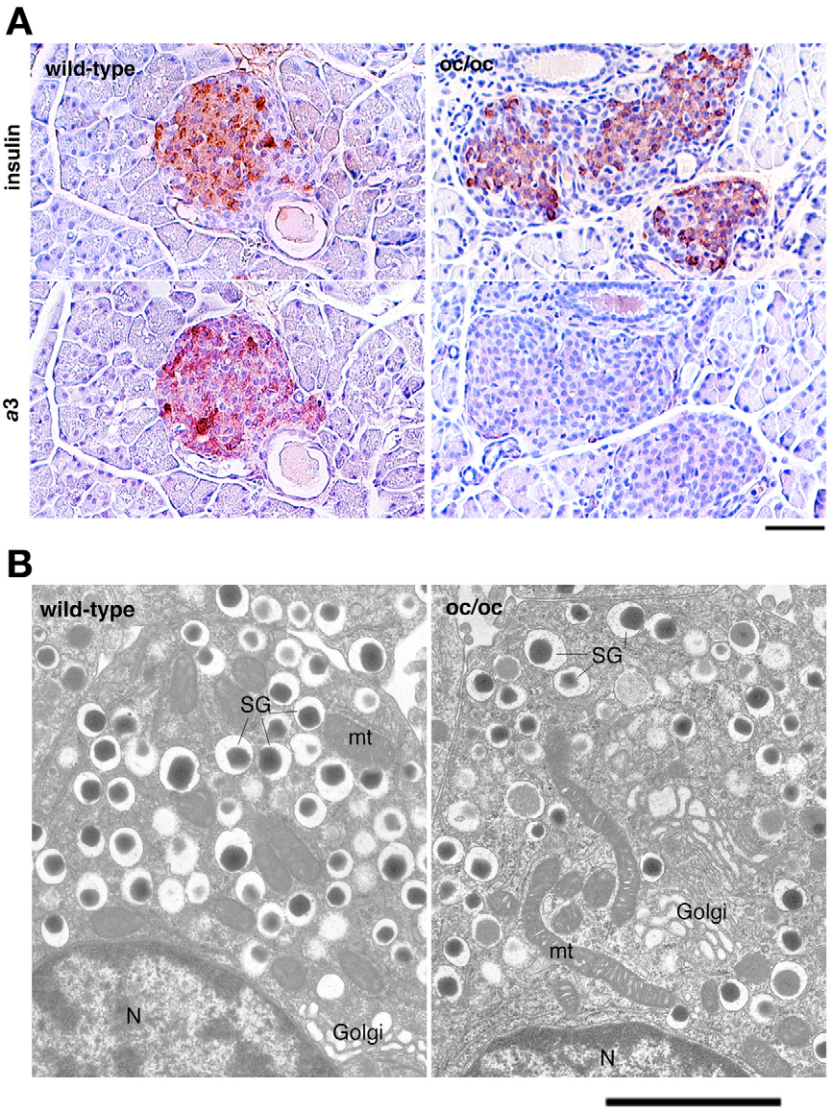

Fig. 6. Immunohistochemistry of the pancreatic islet of *oc/oc* mice with anti-*a*3 and anti-insulin antibodies. (A) Paraffin sections of pancreatic islets from wild-type and *oc/oc* mice were stained with anti-insulin and anti-*a*3 antibodies. The morphologies and sizes of islets in wild-type and *oc/oc* mice were indistinguishable. The insulin contents of β-cells in the islets were comparable. The lack of *a*3 expression in *oc/oc* islets was also confirmed. Bar, 50 μm. (B) Electron micrographs of representative areas of β-cells from wild-type and *oc/oc* mice are shown. The dense-core secretory granules (SG) are indicated. Golgi, Golgi apparatus; mt, mitochondria. Bar, 1 μm.

as driving forces for numerous secondary transport processes (Nelson and Harvey, 1999; Stevens and Forgac, 1997; Sun-Wada et al., 2003). The genetic loss of a common subunit of V-ATPase (the 16 kDa proteolipid) in mice results in growth arrest and defects in organelle morphology in the peri-implantation stage of embryo development, indicating that V-ATPase plays an essential role in mammalian cells. The proteolipid is encoded by a single gene in both humans and mice; thus, since all V-ATPase complexes in a variety of tissues and cells possess this subunit, its genomic disruption results in the loss of function of V-ATPases in whole animals (Sun-Wada et al., 2000). Other subunits, including the large 100 kDa *a* subunit, are encoded by multiple genes, and the diverse intracellular localization of V-ATPase is achieved in part by expressing these distinct isoforms of the membrane-integral *a* subunit (Kawasaki-Nishi et al., 2001; Toyomura et al., 2003).

In this study, we found that one of the *a* isoforms, *a*3, is localized to the membranes of insulin-containing secretory granules in pancreatic β-cells, whereas the other subunit isoforms, *a*1 and *a*2, are localized to the compartments negative for insulin. Therefore, the *a*3 isoform of V-ATPase is specifically targeted to the insulin-containing secretory granules in β-cells. In undifferentiated cells, the *a*3 isoform localizes to late endosomes and lysosomes (Toyomura et al., 2003), and participates in the acidification of these lytic compartments. During differentiation of osteoclasts, which have the *a*3 isoform of V-ATPase on the plasma membrane, the V-ATPase and the lysosomal protein lamp-2 are recruited to the plasma membrane together. In β-cells, *a*3 and lamp-2 are not precisely colocalized within the intracellular compartments. Therefore, the sorting mechanisms for lamp-2 and *a*3 are not the same under different cellular contexts (i.e. differentiating osteoclasts and pancreatic β-cells), and the intracellular sorting events for the V-ATPase isoforms seem to be more complicated than we discussed previously (Toyomura et al., 2003).

Processing of insulin and secretory granule acidification

It has been shown that proinsulin is converted to insulin through the actions of two endopeptidases whose activities are dependent on an acidic pH and the presence of Ca^{2+} (Orci et

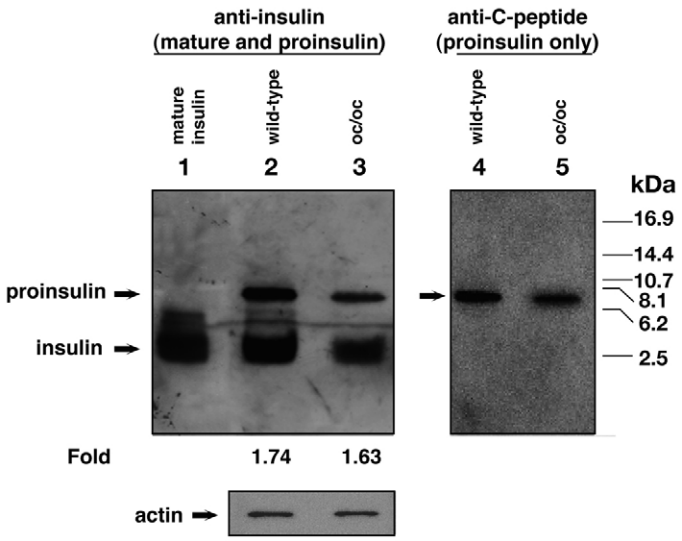

Fig. 7. Immunoblot analysis of insulin processing. Equal amounts of islet protein prepared from either wild-type (lanes 2 and 4) or *oc/oc* homozygous mice (lanes 3 and 5) were subjected to 15-25% gradient polyacrylamide gel electrophoresis in the presence of sodium dodecyl sulfate and 100 mM dithiothreitol. Human insulin was loaded as standard (lane 1). Immunoblotting was performed using anti-insulin or anti-C-peptide antibodies. The positions of a molecular weight marker are shown, and the positions of insulin and proinsulin are indicated (arrows). The intensities of the bands were measured using the image analyzer LAS1000. 'Fold' indicates the ratio of the level of insulin over proinsulin in wild-type or mutant islets.

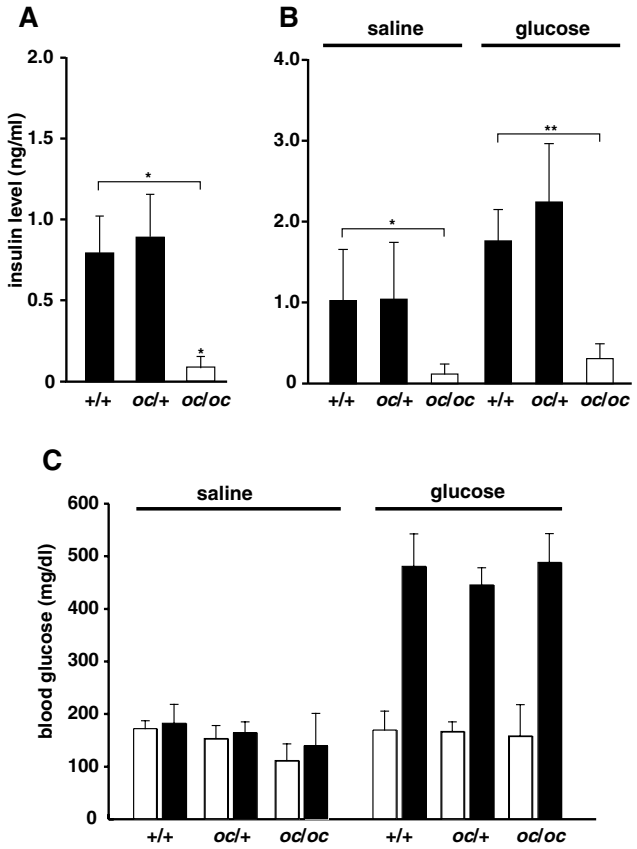

Fig. 8. Plasma insulin levels in *oc/oc* mice. Blood samples were collected from (A) natural-feeding (with a lactating mother and a chew diet) wild-type (+/+; *n*=7), heterozygous (*oc*/+; *n*=8) and *oc/oc* (*n*=7) mice, or (B) fasting (without a lactating mother or a chew diet) mice loaded with glucose [wild-type (+/+; *n*=10), heterozygous (*oc*/+; *n*=10), and *oc/oc* (*n*=10)] or saline [wild-type (+/+; *n*=7), heterozygous (*oc*/+; *n*=7), and *oc/oc* (*n*=3)] (B). Plasma insulin contents were measured by ELISA. (C) The blood glucose levels before (open bar) or after (solid bar) oral administration. The results are presented as means ± s.d. **P*<0.05, compared with wild-type mice; ***P*<0.001, compared with wild-type mice.

al., 1986). The conversion is inhibited by ionophores, which disrupt the intracellular proton gradient (Orci et al., 1986), demonstrating that an acidic environment is necessary for the enzyme reaction in vivo. These results lead us to presume that V-ATPase with the *a*3 isoform might be involved in the conversion of insulin. It was unexpected to find out that the *a*3 isoform or *a*3-mediated acidification is not an absolute requirement for insulin processing. From the immunoblotting analysis and morphology of the dense-core granules observed by electron microscopy, we found that the maturation of insulin was normal in the islets of *oc/oc* mutant mice lacking the *a*3 isoform. In addition, insulin extracted from the *oc/oc* mutant mice had the potential to evoke GLUT-4 translocation in 3T3L1 adipocytes, indicating that this insulin is indistinguishable from that produced in the wild-type mouse in terms of its activities (G.-H.S.-W., unpublished data). The primary site of the conversion, revealed by previous immunoelectron microscopy studies, is clathrin-coated vesicles, which are less acidic than mature secretory granules and more proximal to the Golgi apparatus (Orci et al., 1986; Orci et al., 1987), where the *a*2 isoform is the major constituent for V-ATPase (Toyomura et al., 2003). It is possible that the processing of insulin is carried out in some compartments that are acidified by V-ATPase with other *a* isoforms (e.g. the *a*2 isoform). The expression level of the *a*2 isoform was elevated in the homozygous *oc* mutant (Fig. 5). The localization of *a*2 in mutant β-cells overlapped partially with that of insulin, whereas this ovelapping was not observed in wild-type cells. This upregulation could also be a reason why *oc/oc* mutant mice do not develop severe defects in insulin maturation. In addition, we found that the secretory granules of *oc/oc* mutant β-cells were still stained with an acidotropic reagent, LysoTracker, suggesting that the secretory granules without the *a*3 isoform were acidified to a certain degree. It is possible that the acidification of secretory granules could be compensated by the *a*2 subunit isoform.

The *a* subunit isoform has a regulatory role in secretion

Recently, several lines of studies have reported the requirement of the V-ATPase V_O subunit *a* isoform for exocytosis. The V_O complex has been shown to be required for membrane fusion downstream of SNARE action in a yeast vacuolar fusion (Bayer et al., 2003; Peters et al., 2001). The *a*1 subunit isoform in *Drosophila* has been demonstrated to interact with SNARE proteins and function as a regulator of synaptic vesicle fusion efficiency downstream of SNARE-dependent vesicle priming (Hiesinger et al., 2005). Our results showed that the mutant mice without the *a*3 isoform exhibited a significantly lower level of plasma insulin than the wild-type mice, despite the fact

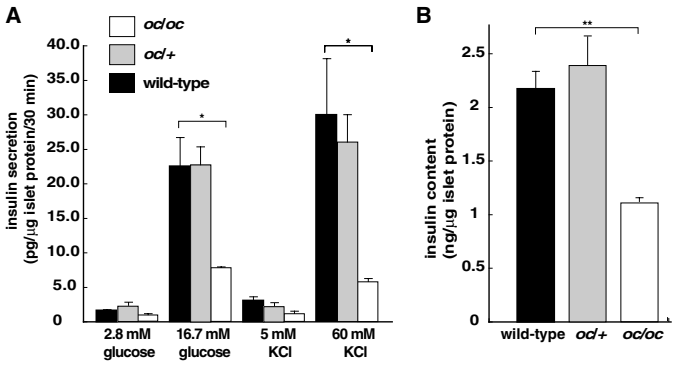

Fig. 9. Secretion of insulin from pancreatic islets. (A) Islets isolated from 2-week-old wild-type (black bars), heterozygous (*oc*/+) (gray bars) and *oc*/*oc* mice (open bars) were incubated under the basal condition for 30 minutes followed by a second 30-minute incubation in the presence of high glucose (16.7 mM) or K^+ (60 mM). Immunoreactive insulin in the media was measured with anti-insulin antibodies and normalized by the protein content in the islet extracts. (B) The islets used in insulin-secretion assays were subsequently extracted with acid-ethanol. The insulin content was calculated per μg islet protein. The results are given as the mean ± s.d. (n=3). *P<0.05, **P<0.005, compared with wild-type mice.

they produced and contained substantial amounts of insulin in the pancreas. Insulin secretion in response to glucose or depolarizing stimulation was significantly impaired in *oc*/*oc* mutant islets. The defects in secretion could be explained, at least in part, by the decrease in insulin content in islets, which was also reduced in the *oc*/*oc* mice. However, the decrease in insulin secretion (~75%) was even lower than the insulin content. These observations suggest that the mutants are defective in the step of exocytosis of secretory granules. Analysis of the effect of bafilomycin treatment on insulin secretion using βHC9 cells supported the idea that insulin secretion might be dependent on the physical presence of the V-ATPase subunit.

The blood glucose levels of *oc*/*oc* mutants were not significantly affected, although the insulin levels were low. In addition, *oc*/*oc* mice do not develop any apparent sign of hyperglycemia as shown in Fig. 8C. As shown in Figs 2 and 3, the *a*3 isoform was also expressed in glucagon-secreting cells. We have also measured the secretion of glucagons from isolated islets and found that their secretion from mutant islets was also impaired (G.-H.S.-W., M.F. and Y.W., unpublished data). Requirement of *a*3 function in glucagon secretion might be an explanation for the lack of apparent hyperglycemia. The expression of the *a*3 isoform is not restricted to the pancreas or osteoclasts, thus the *oc* mutation affects many other cellular and tissue functions in the whole animal. Indeed, we and others noted that the *oc*/*oc* mutation affects animal physiology severely, and the mutant animals exhibit growth retardation (Li et al., 1999; Scimeca et al., 2000; Steward, 2003) and abnormal behavior (our unpublished observation), and cannot survive more than a month after birth. We found that the *a*3 isoform is strongly expressed in secretory cells in various organs, including the adrenal gland, parathyroid gland, pituitary gland and pineal gland (G.-H.S.-W., M.F. and Y.W., unpublished data), which all have essential endocrine functions to maintain whole animal homeostasis. The apparent discrepancy in the blood insulin and glucose levels in *oc*/*oc* mutants might be reflecting deregulated endocrine homeostasis. In addition, the mutants and their normal littermates are highly likely to take different qualities and quantities of diet (normal chew or mother milk, etc.) because *oc*/*oc* mutants are defective in tooth development, which takes place around two weeks after birth (Li et al., 1999) in the normal littermates. The mutant mice could be distinguished easily from the heterozygous or wild-type littermates at a glance by their small sizes and their lack of incisor eruption. Their blood glucose levels reflect these differences in gross physiological parameters.

Several lines of studies for human insulin-dependent (type 1) diabetes mellitus (IDDM) have identified susceptibility regions on human chromosomes. The human V-ATPase *a*3 isoform, encoded by the *ATP6i* gene, was mapped to chromosome 11q13, a region that has been linked to IDDM4 (Davies et al., 1994; Hashimoto et al., 1994). Several positional candidates including *FADD*, *GALN* (Eckenrode et al., 2000) and *LRP5* (Twells et al., 2003) have been investigated, although the functional candidate gene has not been identified yet. The *ATP6i* gene, also designated as *TCIRG1*, is located approximately 200 kb apart from the *LRP5* locus, which shows strong linkage to the disease (Twells et al., 2003). Our results raise the possibility that genetic alteration(s) of the gene encoding human *a*3 could also contribute to IDDM.

Materials and Methods

Materials and animals

Antibodies against subunit *a* isoforms were prepared as described previously (Toyomura et al., 2003; Toyomura et al., 2000). Polyclonal anti-*A* antibodies (WAKO), and monoclonal antibodies for lamp-2 (rat clone GL2A7; DSHB), actin (mouse AC-15; Abcam), and GM130 (mouse clone 35; Harlan Sera-Lab) were used in the experiments. The anti-insulin and C-peptide antibodies were obtained from DAKO and Linco, respectively. Other materials were also from commercial sources: fluorescein isothiocyanate (FITC)- and Cy3-conjugated secondary antibodies were from Jackson ImmunoResearch; Dulbecco's modified Eagle medium (DMEM), minimal essential medium (MEM) and fetal bovine serum (FBS) were from Invitrogen; and recombinant mouse insulin was from Seikagaku Kogyo.

C57Bl/6J-C3H/FeJ F1 *oc*/+ mice were obtained from the Jackson Laboratory (Schlager and Dickie, 1967; Scimeca et al., 2000). Heterozygous *oc*/+ mice were identified by genotyping analysis and homozygous *oc*/*oc* mice were obtained through heterozygous mating. C57Bl/6J mice were purchased from SLC Japan. All animal experiments were carried out in accordance with institutional policies.

Genotyping

Tail DNA prepared by phenol-chloroform extraction was subjected to semi-nested PCR. The wild-type allele was detected as a 2.3 kb product using primers OC-Fw (5′-TATAGTAAGTGGACTGT-3′) and OC-Rv (5′-CTCATTCCATGGGATGTGA-ATCTG-3′). The *oc* allele was detected as a 0.52 kb product with primers OC-mid (5′-ATCATGGGCTCTATGTTCCGGAGT-3′) and OC-Rv.

Western blot analysis

A mouse pancreas was dissected at 4°C. Lysate preparation and immunoblotting procedures were performed as previously described (Sun-Wada et al., 2002). For analysis of insulin processing, the islet total lysates were applied at 5 μg/lane on 15-25% gradient polyacrylamide gel (Daiich Pure Chemicals) and transferred to PVDF membrane with 0.2 μm pore size. The immunoblots were performed with anti-insulin and c-peptide antibodies. The protein blot was developed with an ECL detection kit (GE Healthcare), and images were obtained using an image capture system (model LAS1000; Fujifilm). The intensities of bands were measured and analyzed using Image Gauge Software (Fujifilm).

Cell culture

βHC9 cells (Noda et al., 1996; Radvanyi et al., 1993), a kind gift from D. Hanahan (University of California, San Francisco, CA), were grown in DMEM containing 15% horse serum, 2.5% FBS, 1 mM pyruvate and 25 mM glucose. βTC6 cells (Poitout et al., 1995) obtained from the American Type Culture Collection (ATCC)

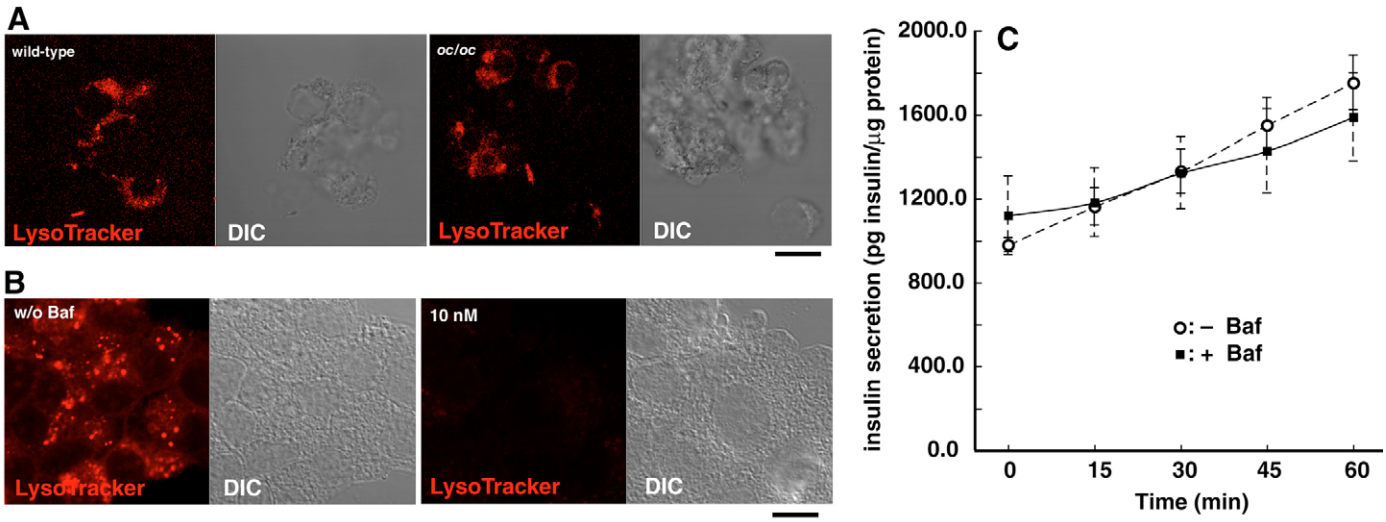

Fig. 10. Acidification of *oc*/*oc* mutant pancreatic islet cells, and insulin secretion in βHC9 cells following treatment with bafilomycin A. (A) Wild-type and *oc*/*oc* islets were dispersed with trypsin and stained with LysoTracker. After fixation with 4% paraformaldehyde in PBS (pH 7.4), the cells were mounted for observation. Bar, 10 μm. (B) LysoTracker staining of control βHC9 (w/o Baf) cells or βHC9 cells after treatment for 1 hour with bafilomycin A (10 nM). Bar, 10 μm. (C) Insulin secretion of βHC9 cells stimulated by 25 mM glucose after treatment for 1 hour with bafilomycin A (10 nM) as described under 'Materials and Methods'. Means ± s.d. of triplicate observations in a single representative experiment are shown here. Broken line and open circle, control cells; solid line and filled square, cells treated with bafilomycin A.

were grown in DMEM containing 15% FBS, 4 mM glutamate and 25 mM glucose, and maintained at 37°C under 5% CO_2.

Immunohistochemistry

The immunnofluorescence of cultured cells were performed as previously described (Toyomura et al., 2003). Fluorescence images were acquired with a confocal microscope, LSM 510 (Carl Zeiss). To stain the islets of Langerhans, mice (C57Bl/6J male; 6 weeks old) were anesthetized and then perfused with 4% paraformaldehyde in phosphate-buffered saline (PBS) (pH 7.4). Each pancreas was dissected out, and then successively infiltrated with 30% sucrose in PBS, embedded in OCT compound (Miles), and stored frozen. Sections of 6 μm thickness were mounted on gelatin-coated slides, and then stained with hematoxylin. Sections were stained immunochemically as described previously (Sun-Wada et al., 2002).

Oral glucose administration and insulin measurement

Mice (*oc*/*oc*, *oc*/+ and +/+; 3 weeks old) were fasted for 4 hours and were then administered glucose through a stomach tube (1.5 mg/g body wt intragastrical administration). Blood was collected in heparinized tubes 10 minutes after glucose administration. Blood glucose was measured using an automatic blood glucose meter (Glutest Ace; Sanea Chemicals). Insulin levels were measured with an enzyme-linked immunosorbent assay (ELISA) kit (Morinaga or Shibayagi) using a mouse insulin standard (Seikagaku Kogyo).

Islet isolation and in vitro secretion assay

Islets were isolated as previously described (Kasai et al., 2005; Wang et al., 1999) with several modifications. Briefly, the pancreas was dissected from 3-week-old mice, digested in 500 U/ml of collagenase solution (Type XI; Sigma-Aldrich) for 30 minutes at 37°C with shaking several times during incubation. Islets were picked up by hand selection under a dissecting microscope and cultured overnight in RPMI1640 (11 mM glucose) supplemented with 10% fetal calf serum, 100 units/ml penicillin and 100 μg/ml streptomycin. Then, 10 islets were transferred into a microfuge tube and incubated for 30 minutes in modified Krebs-Ringer buffer (Kasai et al., 2005) [120 mM NaCl, 5 mM KCl, 24 mM $NaHCO_3$, 1 mM $MaCl_2$, 2 mM $CaCl_2$, 15 mM HEPES (pH 7.4) and 0.1% BSA]. The islets were then incubated at the same buffer for 30 minutes, followed by 30 minutes in the buffer containing secretagogues (16.7 mM glucose or 60 mM KCl). At the time of each medium change, the islets were sedimented by centrifuged at 700 ***g*** for 5 minutes, and media were collected and again centrifuged for 5 minutes to remove any cell debris. Immunoreactive insulin was measured using ELISA (Shibayagi). For γ-aminobutyric acid (GABA) assay, isolated islets were precultured overnight in RPMI1640 (11 mM glucose) supplemented with 10% fetal calf serum, 100 units/ml penicillin and 100 μg/ml streptomycin. Then, 30 islets were cultured for 15 hours in Ham's F-10 medium (Invitrogen) supplemented with 2 mM glutamine, 6.1 mM glucose, 0.2% (wt/vol) charchol-extracted BSA (Type V; Sigma). GABA in the cultured media was measured by HPLC (Smolders et al., 1995).

For bafilomycin A inhibitory experiments, the βHC9 cells were cultured in 12-well plates in DMEM. Each well was washed with 1 ml of PBS and then incubated in DMEM with or without 10 nM bafilomycin at 37°C for 1 hour. Glucose was then added to each well to a final concentration of 25 mM. The medium was collected, centrifuged at 3500 ***g*** for 2 minutes, and the supernatant was collected and stored at –20°C until ELISA assay for insulin. The bafilomycin-treated or control cells were stained with LysoTracker (Molecular Probes) for 15 minutes, and fixed with with 4% paraformaldehyde in PBS (pH 7.4). Fluorescence images were acquired with a confocal microscope, LSM 510 (Carl Zeiss).

Total insulin content

The islet was extracted in an acid-ethanol solution (70% ethanol and 0.18 M HCl) and then sonicated for 20 seconds. The immunoreactive insulin in the supernatant was measured using ELISA (Shibayagi). The acid-ethanol extraction was precipitated with 10% trichloroacetic acid (TCA) (final concentration of TCA was 5%) and the total protein concentration was measured using the BCA Protein Assay (Pierce).

Conventional and immunogold electron microscopy

Conventional electron microscopy was performed as previously described (Sun-Wada et al., 2000). Ultra-thin sections were doubly stained with uranylacetate and lead citrate, and then observed under a Hitachi H7000 electron microscope. The densities of secretory granules were measured and analyzed using Image Gauge software (Fujifilm). For immunoelectron microscopy, the pre-embedded silver enhancement immunogold method was used (Nakamura et al., 2000). A pancreas was fixed in 4% paraformaldehyde in PBS overnight at 4°C. Cryo-sections (6 μm) were incubated with the primary antibodies overnight, followed by incubation with the secondary antibodies conjugated with colloidal gold (1.4 nm diameter). The gold labeling was intensified using a silver enhancement kit (Nano Probes). The quantification of the gold particle distribution was performed in representative sections of a number of cells (n=6).

We thank A. Fukuyama and Y. Takenaka for the expert technical assistance. We are also grateful to H. Okamoto, S. Takasawa, T. Izumi, K. Kasai and K. Yasuda for the helpful discussions throughout this study. This research was supported in part by Grants-in-Aid from the Ministry of Education, Culture, Sports, Science and Technology of Japan, and the Hayashi, Takeda and Noda Foundations.

References

Al-Awqati, Q. (1986). Proton-translocating ATPases. *Annu. Rev. Cell Biol.* **2**, 179-199.
Anraku, Y. (1996). Structure and function of the yeast vacuolar membrane H^+ATPase.

In *Handbook of Biological Physics.* Vol. 2 (ed. J. S. Lolkema), pp. 99-109. Amsterdam: Elsevier Science.

Arvan, P. and Castle, J. D. (1986). Isolated secretion granules from parotid glands of chronically stimulated rats possess an alkaline internal pH and inward-directed H^+ pump activity. *J. Cell Biol.* **103**, 1257-1267.

Barg, S., Huang, P., Eliasson, L., Nelson, D. J., Obermuller, S., Rorsman, P., Thevenod, F. and Renstrom, E. (2001). Priming of insulin granules for exocytosis by granular Cl^- uptake and acidification. *J. Cell Sci.* **114**, 2145-2154.

Bayer, M. J., Reese, C., Buhler, S., Peters, C. and Mayer, A. (2003). Vacuole membrane fusion: V_0 functions after trans-SNARE pairing and is coupled to the Ca^{2+}-releasing channel. *J. Cell Biol.* **162**, 211-222.

Burgess, T. L. and Kelly, R. B. (1987). Constitutive and regulated secretion of proteins. *Annu. Rev. Cell Biol.* **3**, 243-293.

Davies, J., Kawaguchi, Y., Bennett, S. T., Copeman, J. B., Cordell, H. J., Pritchard, L. E., Reed, P. W., Gough, S. C., Jenkins, S. C., Palmer, S. M. et al. (1994). A genome-wide search for human type 1 diabetes susceptibility genes. *Nature* **371**, 130-136.

Eckenrode, S., Marron, M. P., Nicholls, R., Yang, M. C., Yang, J. J., Guida Fonseca, L. C. and She, J. X. (2000). Fine-mapping of the type 1 diabetes locus (IDDM4) on chromosome 11q and evaluation of two candidate genes (FADD and GALN) by affected sibpair and linkage-disequilibrium analyses. *Hum. Genet.* **106**, 14-18.

Futai, M., Oka, T., Sun-Wada, G.-H., Moriyama, Y., Kanazawa, H. and Wada, Y. (2000). Luminal acidification of diverse organelles by V-ATPase in animal cells. *J. Exp. Biol.* **203**, 107-116.

Granger, B. L., Green, S. A., Gabel, C. A., Howe, C. L., Mellman, I. and Helenius, A. (1990). Characterization and cloning of lgp110, a lysosomal membrane glycoprotein from mouse and rat cells. *J. Biol. Chem.* **265**, 12036-12043.

Hashimoto, L., Habita, C., Beressi, J. P., Delepine, M., Besse, C., Cambon-Thomsen, A., Deschamps, I., Rotter, J. I., Djoulah, S., James, M. R. et al. (1994). Genetic mapping of a susceptibility locus for insulin-dependent diabetes mellitus on chromosome 11q. *Nature* **371**, 104-105.

Hayami, K., Noumi, T., Inoue, H., Sun-Wada, G., Yoshimizu, T. and Kanazawa, H. (2001). The murine genome contains one functional gene and two pseudogenes coding for the 16 kDa proteolipid subunit of vacuolar H^+-ATPase. *Gene* **273**, 199-206.

Hayashi, M., Yamamoto, A., Yatsushiro, S., Yamada, H., Futai, M., Yamaguchi, A. and Moriyama, Y. (1998). Synaptic vesicle protein SV2B, but not SV2A, is predominantly expressed and associated with microvesicles in rat pinealocytes. *J. Neurochem.* **71**, 356-365.

Hiesinger, P. R., Fayyazuddin, A., Mehta, S. Q., Rosenmund, T., Schulze, K. L., Zhai, R. G., Verstreken, P., Cao, Y., Zhou, Y., Kunz, J. et al. (2005). The v-ATPase V_0 subunit a1 is required for a late step in synaptic vesicle exocytosis in *Drosophila*. *Cell* **121**, 607-620.

Hutton, J. C. (1994). Insulin secretory granule biogenesis and the proinsulin-processing endopeptidases. *Diabetologia* **37**, S48-S56.

James, D. E., Piper, R. C. and Slot, J. W. (1994). Insulin stimulation of GLUT-4 translocation: a model for regulated recycling. *Trends Cell Biol.* **4**, 120-126.

Kasai, K., Ohara-Imaizumi, M., Takahashi, N., Mizutani, S., Zhao, S., Kikuta, T., Kasai, H., Nagamatsu, S., Gomi, H. and Izumi, T. (2005). Rab27a mediates the tight docking of insulin granules onto the plasma membranes during glucose stimulation. *J. Clin. Invest.* **115**, 388-396.

Kawasaki-Nishi, S., Bowers, K., Nishi, T., Forgac, M. and Stevens, T. H. (2001). The amino-terminal domain of the V-ATPase a subunit controls targeting and *in vivo* dissociation and the carboxyl-terminal domain affects coupling of proton transport and ATP hydrolysis. *J. Biol. Chem.* **276**, 47411-47420.

Kontani, K., Moskowitz, I. P. and Rothman, J. H. (2005). Repression of cell-cell fusion by components of the *C. elegans* vacuolar ATPase complex. *Dev. Cell* **8**, 787-794.

Li, Y., Chen, W., Liang, Y., Li, E. and Stashenko, P. (1999). *Atp6i*-deficient mice exhibit severe osteopetrosis due to loss of osteoclast-mediated extracellular acidification. *Nat. Genet.* **23**, 447-451.

Morel, N., Dedieu, J. C. and Philippe, J. M. (2003). Specific sorting of the a1 isoform of the V-H^+ATPase a subunit to nerve terminals where it associates with both synaptic vesicles and the presynaptic plasma membrane. *J. Cell Sci.* **116**, 4751-4762.

Moriyama, Y. and Futai, M. (1990). H^+-ATPase, a primary pump for accumulation of neurotransmitters, is a major constituent of brain synaptic vesicles. *Biochem. Biophys. Res. Commun.* **173**, 443-448.

Moriyama, Y., Yamamoto, A., Yamada, H., Tashiro, Y. and Futai, M. (1996). Role of endocrine cell microvesicles in intercellular chemical transduction. *Biol. Chem. Hoppe Seyler* **377**, 155-165.

Nakamura, N., Lowe, M., Levine, T. P., Rabouille, C. and Warren, G. (1997). The vesicle docking protein p115 binds GM130, a *cis*-Golgi matrix protein, in a mitotically regulated manner. *Cell* **89**, 445-455.

Nakamura, N., Yamamoto, A., Wada, Y. and Futai, M. (2000). Syntaxin 7 mediates endocytic trafficking to late endosomes. *J. Biol. Chem.* **275**, 6523-6529.

Nelson, N. (1993). Presynaptic events involved in neurotransmission. *J. Physiol. Paris* **87**, 171-178.

Nelson, N. and Harvey, W. R. (1999). Vacuolar and plasma membrane proton-adenosinetriphosphatases. *Physiol. Rev.* **79**, 361-385.

Nishi, T. and Forgac, M. (2000). Molecular cloning and expression of three isoforms of the 100-kDa a subunit of the mouse vacuolar proton-translocating ATPase. *J. Biol. Chem.* **275**, 6824-6830.

Nishi, T. and Forgac, M. (2002). The vacuolar H^+-ATPase – Nature's most versatile proton pump. *Nat. Rev. Mol. Cell Biol.* **3**, 94-103.

Noda, M., Komatsu, M. and Sharp, G. W. (1996). The βHC-9 pancreatic β-cell line preserves the characteristics of progenitor mouse islets. *Diabetes* **45**, 1766-1773.

Oka, T., Murata, Y., Namba, M., Yoshimizu, T., Toyomura, T., Yamamoto, A., Sun-Wada, G.-H., Hamasaki, N., Wada, Y. and Futai, M. (2001). *a*4, a unique kidney-specific isoform of mouse vacuolar H^+-ATPase subunit *a*. *J. Biol. Chem.* **276**, 40050-40054.

Orci, L., Ravazzola, M., Amherdt, M., Madsen, O., Perrelet, A., Vassalli, J. D. and Anderson, R. G. (1986). Conversion of proinsulin to insulin occurs coordinately with acidification of maturing secretory vesicles. *J. Cell Biol.* **103**, 2273-2281.

Orci, L., Ravazzola, M., Storch, M. J., Anderson, R. G., Vassalli, J. D. and Perrelet, A. (1987). Proteolytic maturation of insulin is a post-Golgi event which occurs in acidifying clathrin-coated secretory vesicles. *Cell* **49**, 865-868.

Orci, L., Halban, P., Perrelet, A., Amherdt, M., Ravazzola, M. and Anderson, R. G. (1994). pH-independent and -dependent cleavage of proinsulin in the same secretory vesicle. *J. Cell Biol.* **126**, 1149-1156.

Peters, C., Bayer, M. J., Buhler, S., Andersen, J. S., Mann, M. and Mayer, A. (2001). *Trans*-complex formation by proteolipid channels in the terminal phase of membrane fusion. *Nature* **409**, 581-588.

Poitout, V., Stout, L. E., Armstrong, M. B., Walseth, T. F., Sorenson, R. L. and Robertson, R. P. (1995). Morphological and functional characterization of βTC-6 cells–an insulin-secreting cell line derived from transgenic mice. *Diabetes* **44**, 306-313.

Radvanyi, F., Christgau, S., Baekkeskov, S., Jolicoeur, C. and Hanahan, D. (1993). Pancreatic β cells cultured from individual preneoplastic foci in a multistage tumorigenesis pathway: a potentially general technique for isolating physiologically representative cell lines. *Mol. Cell. Biol.* **13**, 4223-4232.

Schlager, G. and Dickie, M. M. (1967). Spontaneous mutations and mutation rates in the house mouse. *Genetics* **57**, 319-330.

Scimeca, J. C., Franchi, A., Trojani, C., Parrinello, H., Grosgeorge, J., Robert, C., Jaillon, O., Poirier, C., Gaudray, P. and Carle, G. F. (2000). The gene encoding the mouse homologue of the human osteoclast-specific 116-kDa V-ATPase subunit bears a deletion in osteosclerotic (*oc/oc*) mutants. *Bone* **26**, 207-213.

Smeekens, S. P., Montag, A. G., Thomas, G., Albiges-Rizo, C., Carroll, R., Benig, M., Phillips, L. A., Martin, S., Ohagi, S., Gardner, P. et al. (1992). Proinsulin processing by the subtilisin-related proprotein convertases furin, PC2, and PC3. *Proc. Natl. Acad. Sci. USA* **89**, 8822-8826.

Smith, A. N., Finberg, K. E., Wagner, C. A., Lifton, R. P., Devonald, M. A., Su, Y. and Karet, F. E. (2001). Molecular cloning and characterization of *Atp6n1b*: a novel fourth murine vacuolar H^+-ATPase *a*-subunit gene. *J. Biol. Chem.* **276**, 42382-42388.

Smolders, A., Schuit, F., Michotte, Y. and Ebinger, G. (1995). The analysis of excitatory, inhibitory and other amino acids in rat brain microdialysates using microbore liquid chromatography. *J. Neurosci. Methods* **57**, 47-53.

Stevens, T. H. and Forgac, M. (1997). Structure, function and regulation of the vacuolar (H^+)-ATPase. *Annu. Rev. Cell Dev. Biol.* **13**, 779-808.

Steward, C. G. (2003). Neurological aspects of osteopetrosis. *Neuropathol. Appl. Neurobiol.* **29**, 87-97.

Sun-Wada, G.-H., Murata, Y., Yamamoto, A., Kanazawa, H., Wada, Y. and Futai, M. (2000). Acidic endomembrane organelles are required for mouse postimplantation development. *Dev. Biol.* **228**, 315-325.

Sun-Wada, G.-H., Murakami, H., Nakai, H., Wada, Y. and Futai, M. (2001). Mouse *Atp6f*, the gene encoding the 23-kDa proteolipid of vacuolar proton translocating ATPase. *Gene* **274**, 93-99.

Sun-Wada, G.-H., Imai-Senga, Y., Yamamoto, A., Murata, Y., Hirata, T., Wada, Y. and Futai, M. (2002). A proton pump ATPase with testis-specific *E*1 subunit isoform required for acrosome acidification. *J. Biol. Chem.* **277**, 18098-18105.

Sun-Wada, G.-H., Wada, Y. and Futai, M. (2003). Vacuolar H^+ pumping ATPases in luminal acidic organelles and extracellular compartments: common rotational mechanism and diverse physiological roles. *J. Bioenerg. Biomembr.* **35**, 347-358.

Toyomura, T., Oka, T., Yamaguchi, C., Wada, Y. and Futai, M. (2000). Three subunit *a* isoforms of mouse vacuolar H^+-ATPase. Preferential expression of the *a*3 isoform during osteoclast differentiation. *J. Biol. Chem.* **275**, 8760-8765.

Toyomura, T., Murata, Y., Yamamoto, A., Oka, T., Sun-Wada, G.-H., Wada, Y. and Futai, M. (2003). From lysosomes to plasma membrane: localization of vacuolar type H^+-ATPase with the *a*3 isoform during osteoclast dfferentiation. *J. Biol. Chem.* **278**, 22023-22030.

Twells, R. C., Mein, C. A., Payne, F., Veijola, R., Gilbey, M., Bright, M., Timms, A., Nakagawa, Y., Snook, H., Nutland, S. et al. (2003). Linkage and association mapping of the LRP5 locus on chromosome 11q13 in type 1 diabetes. *Hum. Genet.* **113**, 99-105.

Unno, M., Nata, K., Noguchi, N., Narushima, Y., Akiyama, T., Ikeda, T., Nakagawa, K., Takasawa, S. and Okamoto, H. (2002). Production and characterization of Reg knockout mice: reduced proliferation of pancreatic β-cells in Reg knockout mice. *Diabetes* **51**, S478-S483.

Urbe, S., Dittie, A. S. and Tooze, S. A. (1997). pH-dependent processing of secretogranin II by the endopeptidase PC2 in isolated immature secretory granules. *Biochem. J.* **321**, 65-74.

Uthayakumar, S., Granger, B. L., Green, S. A., Gabel, C. A., Howe, C. L., Mellman, I. and Helenius, A. (1990). Cell surface accumulation of overexpressed hamster lysosomal membrane glycoproteins: characterization and cloning of lgp110, a lysosomal membrane glycoprotein from mouse and rat cells. *J. Biol. Chem.* **265**, 405-420.

Wang, J., Takeuchi, T., Tanaka, S., Kubo, S., Kayo, T., Lu, D., Takta, K., Koizumi, A. and Izumi, T. (1999). A mutation in the insulin 2 gene induces diabetes with severe pancreatic β-cell dysfunction in the *Mody* mice. *J. Clin. Invest.* **103**, 27-37.

Weisz, O. A. (2003). Acidification and protein traffic. *Int. Rev. Cytol.* **226**, 259-319.